Biochemical and Biophysical Research Communications xxx (2017) 1–6

Contents lists available at ScienceDirect

Biochemical and Biophysical Research Communications

journal homepage: www.elsevier.com/locate/ybbrc

Thermodynamic contribution of backbone conformational entropy in the binding between SH3 domain and proline-rich motif

Danyun Zeng, Qingliang Shen, Jae-Hyun Cho*

Department of Biochemistry and Biophysics, Texas A&M University, College Station, TX 77843, USA

ARTICLE INFO

Article history:
Received 13 January 2017
Accepted 18 January 2017
Available online xxx

Keywords:
Intrinsically disordered proteins
Conformational entropy
SH3 domain
Proline-rich motif
Protein-protein interactions

ABSTRACT

Biological functions of intrinsically disordered proteins (IDPs), and proteins containing intrinsically disordered regions (IDRs) are often mediated by short linear motifs, like proline-rich motifs (PRMs). Upon binding to their target proteins, IDPs undergo a disorder-to-order transition which is accompanied by a large conformational entropy penalty. Hence, the molecular mechanisms underlying control of conformational entropy are critical for understanding the binding affinity and selectivity of IDPs-mediated protein-protein interactions (PPIs). Here, we investigated the backbone conformational entropy change accompanied by binding of the N-terminal SH3 domain (nSH3) of CrkII and PRM derived from guanine nucleotide exchange factor 1 (C3G). In particular, we focused on the estimation of conformational entropy change of disordered PRM upon binding to the nSH3 domain. Quantitative characterization of conformational dynamics of disordered peptides like PRMs is limited. Hence, we combined various methods, including NMR model-free analysis, δ2D, DynaMine, and structure-based calculation of entropy loss. This study demonstrates that the contribution of backbone conformational entropy change is significant in the PPIs mediated by IDPs/IDRs.

1. Introduction

PPIs via IDPs or IDRs play critical roles in diverse biological processes, such as regulation of gene transcription [1,2] and signal transduction [3–5]. Many IDPs/IDRs undergo folding or disorder-to-order transition upon binding to their target proteins or membrane [6–10]. Hence, binding of IDPs to target proteins is assumed to be accompanied by a large loss of conformational entropy [11–13]. To overcome this entropy penalty, IDPs/IDRs can increase the favorable enthalpy by expanding the binding surface area, or reduce the conformational entropy by retaining flexibility (often called “fuzziness”) in the bound state [14].

PRM is one of the most common short linear motif found in IDPs/IDRs [15,16]. A large number of PRMs bind to the SH3 domain. Hence, the interactions between PRMs and SH3 domains are archetypal PPIs mediated by IDPs/IDRs. The thermodynamic signature of SH3:PRM interactions highlights the complexity of the interplay between the desolvation and conformational entropy [17–19]. Changes in the solvent accessible surface area indicate that SH3:PRM interactions would be driven by entropy, owing to desolvation of the hydrophobic binding interface [17–20]. Nonetheless, the binding entropy was measured to be unfavorable in many SH3:PRM complexes [17–19]. This contradictory result implies that a large amount of conformational entropy change is associated with binding of SH3 domain and PRM [17,19,21,22].

It has often been assumed that PRMs undergo a minor conformational change upon binding to SH3 domains because of high type II poly-proline (PPII) helix propensities. However, PPII helix propensities of PRMs can be very low [23], and vary widely according to their sequences. Furthermore, backbone conformational entropy change can be significantly large, even if the PPII propensity of PRM is high [17,21,22]. Here, we estimated the backbone conformational entropy changes of both nSH3 domain and PRM derived from C3G (PRM^{C3G}) upon binding. Our results support the notion that backbone conformational entropy contributes considerably to the binding thermodynamics of PRM.

2. Materials and methods

2.1. Sample preparation

The protein samples used in this study were prepared as

* Corresponding author.
E-mail address: jaehyuncho@tamu.edu (J.-H. Cho).

http://dx.doi.org/10.1016/j.bbrc.2017.01.089
0006-291X/

described previously [19]. The PRM^{C3G} used in this study was prepared using *E.* coli BL21 (DE3) expression system with a plasmid containing a gene for the PRM^{C3G} (residues 282 to 291) of human C3G. For purification and quantitation purposes, one Gly and Tyr were added to the N- and C-terminus, respectively. The expressed PRM was purified using N-sepharose and digested with SUMO protease to remove N-terminal SUMO-tag. The PRM was further purified using HPLC.

2.2. Binding assay

The dissociation constant, K_d, of nSH3:PRM complex was measured by monitoring the change of tryptophan fluorescence signal, as described previously [19].

2.3. NMR resonance assignment

All NMR experiments were conducted using protein samples in 20 mM sodium phosphate (pH 6.1), 80 mM NaCl, 0.02% sodium azide, 1 mM EDTA, 10 μM DSS (4,4-dimethyl-4-silapentane-sulfonate), and 10% D_2O at 25 °C. The assignment of ^{1}H, ^{13}C, and ^{15}N resonances was carried as described previously [24]. ^{1}H chemical shifts were referenced with respect to DSS, and ^{13}C and ^{15}N chemical shifts were referenced indirectly [25].

2.4. δ2D calculation

To calculate the secondary structure populations in the free PRM, we used δ2D server (http://www-mvsoftware.ch.cam.ac.uk) (Supplementary Table 1). The list of chemical shifts used in the δ2D calculation is shown in the supplementary information (Supplementary Table 2).

2.5. Model free analysis

All relaxation experiments were conducted at 11.8 T and 14.1 T Bruker Avance spectrometer at 25 °C, as described previously [19]. R_1, R_2, and heteronuclear NOE were analyzed according to Lipari-Szabo model free formalism [26,27] using the softwares 'Modelfree version 4.20' [28] and 'FAST-Modelfree' [29]. All Modelfree calculations used $r_{NH} = 1.02$ Å and ^{15}N CSA = −160 ppm. The choice of r_{NH} and CSA values affect the calculated order parameter (O^2) thorough the consideration of the zero-point librations [30,31]. However, this does not affect the comparison of O2 values between the free and complex states. An isotropic diffusion model was used for analysis of the free nSH3 domain, with $t_m = 6.18$ ns. An axially symmetric diffusion tensor, with $t_m = 7.05$ ns and $D_r = 1.37$, was used for analysis of the nSH3:PRM^{C3G} complex. The t_m values seem slightly larger than the expected values for the similar size of proteins. However, this is due to that the construct of the nSH3 domain includes two disordered tails in the N (residues 125−134) and the C (residues 191 − 207) termini.

2.6. Structure of nSH3:PRM^{C3G} complex

Initial docking of the nSH3 domain and PRM^{C3G} was performed using high ambiguity driven biomolecular docking (HADDOCK) method [32,33]. Active residues in the protein were defined as those whose CSP values are larger than one standard deviation from the average. The list of active residues defined by CSP analysis is shown in the Supplementary Information (Supplementary Table 3). Unambiguous distance restraints were obtained from the intermolecular NOESY that were measured using the complex sample of non-isotope labeled nSH3 domain and ^{15}N labeled PRM^{C3G}. The list of intermolecular NOESY cross-peaks is shown in Supplementary Table 4. R_2/R_1 ratio of both nSH3 and PRM^{C3G} and torsion angles predicted by TALOS-N [34] were used as additional restraints in the docking. The top-ranked complex structure from HADDOCK simulation was used as an input structure for further structural refinement, using the Rosetta FlexPepDock server [35,36]. The final complex structure used in this study is the top-ranked structure according to the Rosetta energy score [36] used in FlexPepDock.

3. Results

3.1. Binding thermodynamics of nSH3 and PRM^{C3G}

We calculated the binding thermodynamics of the nSH3 domain and PRM^{C3G} using van't Hoff analysis in two different ways [37]: RTln (K_d) vs. T and ln (K_d) vs 1/T (Fig. 1). The ΔH° and ΔS° associated with binding were calculated to be −13.0 ± 0.8 kcal mol^{-1} and −15.5 ± 2.8 cal mol^{-1} K^{-1}, respectively. This indicates that binding of PRM^{C3G} to the nSH3 domain is driven by favorable enthalpy, accompanied by an unfavorable entropy change. The isothermal titration calorimetry experiments also yielded similar binding parameters for other SH3 domains and their cognate PRMs [17,18].

3.2. Structure model of nSH3:PRM^{C3G} complex

NMR order parameter analysis requires the protein structure to account for the anisotropy of the rotational diffusion tensor of a protein [38,39]. The crystal structure of PRM^{C3G} bound nSH3 domain is available (PDB ID: 1CKA) [40]. However, the amino acid sequence of PRM^{C3G} in our study is four amino acids longer than the ligand in the crystal structure. Hence, we determined the structural model of nSH3:PRM^{C3G} complex using HADDOCK and the FlexPepDock server (Fig. 2A and B), as described in Materials and methods. Overall, the calculated structure was highly similar to the crystal structure (PDB ID: 1CKA) (Supplementary Figs. 1 and 2). The N- and C-terminal regions of PRM^{C3G} are conformationally heterogeneous, which is consistent with the crystal structure. The residue number in the PRM^{C3G} follows the notation [41], where ϕ in PxϕPxK motif is designated as P_0 position (ϕ represents

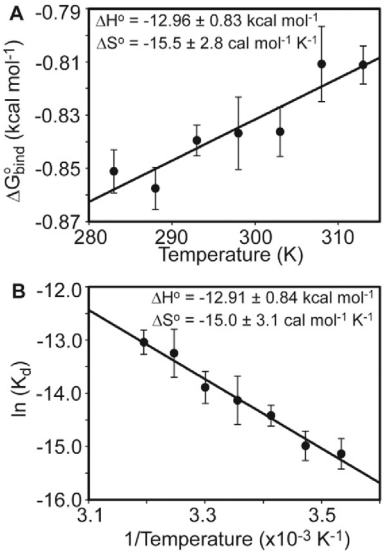

Fig. 1. Van't Hoff plots of the interactions between the nSH3 domain and PRM^{C3G}. (A) Plot of ΔG° vs. T and (B) ln (K_d) vs. 1/T. The solid lines represent the linear regression fit to the data. The calculated thermodynamic parameters are shown in each plot.

Please cite this article in press as: D. Zeng, et al., Thermodynamic contribution of backbone conformational entropy in the binding between SH3 domain and proline-rich motif, Biochemical and Biophysical Research Communications (2017), http://dx.doi.org/10.1016/j.bbrc.2017.01.089